Journal of Visualized Experiments

A Permanent Window for Investigating Cancer Metastasis to the Lung

--Manuscript Draft--

Article Type:	Invited Methods Collection - JoVE Produced Video
Manuscript Number:	JoVE62761R1
Full Title:	A Permanent Window for Investigating Cancer Metastasis to the Lung
Corresponding Author:	Lucia Borriello, PhD Albert Einstein Cancer Center: Albert Einstein Medical Center Bronx, New York UNITED STATES
Corresponding Author's Institution:	Albert Einstein Cancer Center: Albert Einstein Medical Center
Corresponding Author E-Mail:	lucia.borriello@einsteinmed.org
Order of Authors:	David Entenberg
	Lucia Borriello, PhD
	Brian Traub
	Anouchka Coste
	Maja Oktay
	John Condeelis
Additional Information:	
Question	**Response**
Please specify the section of the submitted manuscript.	Cancer Research
Please indicate whether this article will be Standard Access or Open Access.	Standard Access ($1400)
Please indicate the **city, state/province, and country** where this article will be **filmed**. Please do not use abbreviations.	Bronx, NY, US
Please confirm that you have read and agree to the terms and conditions of the author license agreement that applies below:	I agree to the Author License Agreement
Please provide any comments to the journal here.	

TITLE:

A Permanent Window for Investigating Cancer Metastasis to the Lung

AUTHORS AND AFFILIATIONS:

Lucia Borriello[#,1,2], Brian Traub[#,1,2,3], Anouchka Coste[1,3], Maja H. Oktay[1,2,4,5], David Entenberg*[1,2,4]

[1]Department of Anatomy and Structural Biology, Einstein College of Medicine / Montefiore Medical Center, Bronx, NY, USA

[2]Gruss-Lipper Biophotonics Center, Einstein College of Medicine / Montefiore Medical Center, Bronx, NY, USA

[3]Department of Surgery, Einstein College of Medicine / Montefiore Medical Center, Bronx, NY, USA

[4]Integrated Imaging Program, Einstein College of Medicine / Montefiore Medical Center, Bronx, NY, USA

[5]Department of Pathology, Einstein College of Medicine / Montefiore Medical Center, Bronx, NY, USA

[#]co-first authors

Email addresses of co-authors:

Lucia Borriello (lucia.borriello@einsteinmed.org)
Brian Traub (brian.traub@einsteinmed.org)
Anouchka Coste (acoste@atsu.edu)
Maja H. Oktay (moktay@montefiore.org)
David Entenberg (david.entenberg@einsteinmed.org)

*Corresponding authors:

David Entenberg (david.entenberg@einsteinmed.org)

SUMMARY:

Here, we present a protocol for the surgical implantation of a permanently indwelling optical window for the murine thorax, which enables high-resolution, intravital imaging of the lung. The permanence of the window makes it well-suited to the study of dynamic cellular processes in the lung, especially those that are slowly evolving, such as metastatic progression of disseminated tumor cells.

ABSTRACT:

Metastasis, accounting for ~90% of cancer-related mortality, involves the systemic spread of cancer cells from primary tumors to secondary sites such as the bone, brain, and lung. Although extensively studied, the mechanistic details of this process remain poorly understood. While common imaging modalities, including computed tomography (CT), positron emission tomography (PET), and magnetic resonance imaging (MRI), offer varying degrees of gross visualization, each lacks the temporal and spatial resolution necessary to detect the dynamics of individual tumor cells. To address this, numerous techniques have been described for intravital

imaging of common metastatic sites. Of these sites, the lung has proven especially challenging to access for intravital imaging owing to its delicacy and critical role in sustaining life. Although several approaches have previously been described for single-cell intravital imaging of the intact lung, all involve highly invasive and terminal procedures, limiting the maximum possible imaging duration to 6–12 h. Described here is an improved technique for the permanent implantation of a minimally invasive thoracic optical Window for High-Resolution Imaging of the Lung (WHRIL). Combined with an adapted approach to microcartography, the innovative optical window facilitates serial intravital imaging of the intact lung at single-cell resolution across multiple imaging sessions and spanning multiple weeks. Given the unprecedented duration of time over which imaging data can be gathered, the WHRIL can facilitate the accelerated discovery of the dynamic mechanisms underlying metastatic progression and numerous additional biologic processes within the lung.

INTRODUCTION:

Responsible for ~90% of deaths, metastasis is the major cause of cancer-related mortality[1]. Among the major sites of clinically observed metastasis (bone, liver, lung, brain)[2], the lung has proven particularly challenging for *in vivo* imaging via intravital microscopy. This is because the lung is a delicate organ in perpetual motion. The lungs' continuous motion, further compounded by intrathoracic cardiac motion, represents a substantial barrier to accurate imaging. Therefore, due to its relative inaccessibility to modalities for high-resolution intravital optical imaging, cancer growth within the lung has often been deemed an occult process[3].

In the clinical setting, imaging technologies such as computed tomography (CT), positron emission tomography (PET), and magnetic resonance imaging (MRI) enable visualization deep within intact vital organs such as the lung[4]. However, while these modalities provide for excellent views of the gross organ (often even revealing pathology prior to the onset of clinical symptoms), they are of inadequate resolution to detect individual disseminated tumor cells as they advance through the early stages of metastasis. Consequently, by the time the aforementioned modalities provide any indication of metastasis to the lung, metastatic foci are already well established and proliferating. Since the tumor microenvironment plays a pivotal role in cancer progression and metastasis formation[5,6], there is great interest in investigating the earliest steps of metastatic seeding *in vivo*. This interest is further fueled by the increased appreciation that cancer cells disseminate even before the primary tumor is detected[7,8] and the increasing evidence that they survive as single cells and in a dormant state for years to decades before outgrowth into macro-metastasis[9].

Previously, imaging of the lung at single-cell resolution has necessarily involved *ex vivo* or explant preparations[10–13], limiting analyses to single time points. While these preparations do provide useful information, they do not provide any insight into the dynamics of tumor cells within the organ connected to an intact circulatory system.

Recent technological advancements in imaging have enabled intravital visualization of the intact lung at single-cell resolution over periods of up to 12 h[14–16]. This was accomplished in a murine model using a protocol that involved mechanical ventilation, resection of the ribcage, and

vacuum-assisted lung immobilization. However, despite offering the first single cell-resolution images of the physiologically intact lung, the technique is highly invasive and terminal, thereby precluding further imaging sessions beyond the index procedure. This limitation, therefore, prevents its application to the study of metastatic steps that take longer than 12 h, such as dormancy and re-initiation of growth[14–16]. Further still, patterns of cellular behavior observed using this imaging approach must be cautiously interpreted, given that vacuum-induced pressure differentials are likely to cause diversions in blood flow.

To overcome these limitations, a minimally invasive Window for High-Resolution Imaging of the Lung (WHRIL) was recently developed, facilitating serial imaging over an extended period of days to weeks, without the need for mechanical ventilation[17]. The technique entails the creation of a 'transparent ribcage' with a sealed thoracic cavity for the preservation of normal lung function. The procedure is well-tolerated, permitting the mouse to recover without meaningful alteration to baseline activity and function. To reliably localize exactly the same lung region at each respective imaging session, a technique known as microcartography was applied to this window[18]. Through this window, it was possible to capture images of cells as they arrive at the vascular bed of the lung, cross the endothelium, undergo cell division, and grow into micro-metastases.

Here, the study presents a detailed description of an improved surgical protocol for implantation of the WHRIL, which simplifies the surgery while simultaneously increasing its reproducibility and quality. While this protocol was designed to enable investigation of the dynamic processes underlying metastasis, the technique may be alternatively applied to investigations of numerous processes of lung biology and pathology.

PROTOCOL:

All procedures described in this protocol have been performed in accordance with guidelines and regulations for the use of vertebrate animals, including prior approval by the Albert Einstein College of Medicine Institutional Animal Care and Use Committee.

1. Passivation of windows

1.1. Rinse the optical window frames (**Supplemental Figure 2**) with a 1% (w/v) solution of enzymatically-active detergent.

1.2. Inside a glass jar, submerge the optical window frames in 5% (w/v) sodium hydroxide solution for 30 min at 70 °C.

1.3. Remove and wash the window frames with deionized water.

1.4. Inside a new glass jar, submerge the optical window frames in 7% (w/v) citric acid solution for 10 min at 55 °C.

1.5. Again, remove and wash the window frames with deionized water.

1.6. Repeat step 1.2; then, remove and wash window frames with deionized water.

2. Preparation for surgery

2.1. Conduct the surgery in a hood or laminar flow cabinet. To avoid contamination of the operative field, ensure distinct, separated areas for preparation, surgery, and recovery, respectively.

2.2. In advance of the surgery, sterilize all surgical instruments in an autoclave. If subsequent procedures are planned, re-sterilize instruments using a hot bead sterilizer.

2.3. Power on the heated surgical bead and bead sterilizer.

2.4. Anesthetize the mouse with 5% isoflurane in the anesthesia chamber.

2.5. To remove hair, generously apply depilatory cream to the upper-left chest incision site. After no longer than 20 s, firmly wipe away hair and depilatory cream using moistened tissue paper. Repeat as necessary to remove all hair from the surgical site.

2.6. Using 2-0 silk suture, tie a knot at the base of a 22 G catheter, leaving 2-inch long tails (see **Figure 1A**).

3. Lung window surgery

3.1. Wash hands using antiseptic soap.

3.2. Prior to each new surgery, don new sterile gloves.

3.3. To prevent corneal drying and damage to the mouse's eyes, apply ophthalmic ointment to both eyes.

3.4. Dilute 10 µL (0.1 mg/kg) of buprenorphine in 90 µL of sterile PBS, and then inject subcutaneously to ensure preoperative analgesia.

3.5. Intubate the mouse with the silk suture-tied 22 G catheter[15]. Using an inflation bulb, confirm successful intubation by noting bilateral chest rise upon bulb squeeze.

3.6. Secure the intubation catheter by tying the 2-0 silk suture around the mouse's snout (see **Figure 1B**).

3.7. Place the mouse onto the heated surgical stand and position it in the right lateral decubitus to expose the left thorax.

3.8. Connect ventilator to the intubation catheter.

3.9. Ensure controlled, stable ventilation on the ventilator and then lower the isofluorane to 3%. At the procedure's onset and periodically throughout the duration of the procedure, assess the adequacy of anesthesia by performing a toe pinch test.

3.10. Using paper tape, cranially and caudally secure the front and hind limbs, respectively, to the heated surgical stage. Place another piece of tape along the length of the mouse's back to maximize exposure to the surgical field (see **Figure 1C**).

3.11. Open all surgical instruments underneath the hood for the preservation of sterility.

3.12. Sterilize the surgical site by a generous application of antiseptic to the mouse's skin.

3.13. Using forceps, lift the skin and make an ~10 mm circular incision, ~7 mm to the left of the sternum and ~7 mm superior to the subcostal margin (**Figure 1D**).

3.14. Carefully identify any major vessels. If the division of vessels is necessary, cauterize at both ends with the electrocautery pen to maintain hemostasis.

3.15. Excise the soft tissue overlying the ribs.

3.16. Elevate the 6^{th} or 7^{th} rib using forceps. Using a single blade of the blunt micro-dissecting scissors, the rounded side towards the lung, carefully pierce the intercostal muscle between the 6^{th} and 7^{th} ribs to enter the intrathoracic space (**Figure 1E**).

3.17. Delicately discharge compressed air canister at the defect to collapse the lung and separate it from the chest wall. Fire the compressed air in short bursts to prevent iatrogenic lung injury.

3.18. Place the biopsy punch over the cutting tool (**Supplementary Figure 1**) and carefully maneuver the cutting tool's base through the intercostal incision (**Figure 1F**).

3.19. Orient the base of the cutting tool such that it is parallel with the chest wall. Punch a 5 mm circular hole through the rib cage (**Figure 1G**).

NOTE: Ensure that the exposed lung tissue is pink, without signs of damage.

3.20. Using the 5-0 silk suture, create a purse-string stitch ~1 mm from the hole, circumferentially, interlacing with the ribs (**Figure 1H**).

3.21. Position the window frame such that the edges of the circular defect align within the window's groove (see **Figure 1I**).

3.22. Securely lock the implanted window by tightly tying down the 5-0 silk suture.

3.23. Using the 1 mL syringe, draw up ~100 µL of cyanoacrylate gel adhesive.

3.24. Dry the lung by applying a steady gentle stream of compressed air for ~10–20 s (**Figure 1J**).

3.25. Using forceps to grip the window frame by its outside edge, gently lift to ensure separation of the lung from the undersurface of the window frame.

3.26. Dispense a thin layer of cyanoacrylate adhesive along the undersurface of the optical window frame (**Figure 1K**).

3.27. Increase the positive end-expiratory pressure (PEEP) on the ventilator to inflate the lung.

3.28. Holding for 10–20 s, apply gentle but firm pressure to attach the optical window frame onto the lung tissue (**Figure 1L**).

3.29. Dispense a 5 mm drop of the remaining cyanoacrylate gel adhesive onto a rectangular coverslip.

3.30. Pick up the 5 mm coverslip using vacuum pickups. Dip the undersurface of the coverslip into the adhesive, and then scrape off excess adhesive three times against the side of the rectangular coverslip, such that only a very thin layer remains (**Figure 1M**).

3.31. Carefully position the coverslip to fit inside the recess at the center of the optical window frame and is held above the lung tissue at an angle. Briefly clamp the ventilator to generate positive pressure, hyper-inflating the lung. Using a rotating motion, orient the coverslip parallel to the lung tissue to create direct apposition between the lung's surface and the undersurface of the coverslip. Maintain gentle pressure, allowing the cyanoacrylate adhesive to set (~25 s).

3.32. Use the forceps to separate the coverslip from the vacuum pickups (**Figure 1N**).

3.33. Using 5-0 silk suture, again create a purse-string stitch, this time <1 mm circumferentially from the cut-edge of the skin incision. Tuck any excess skin underneath the outer rim of the window frame before tying it down tightly with locking knots.

3.34. To ensure an air-tight seal between the coverslip and the window frame, dispense a small amount of liquid cyanoacrylate at the metal-glass interface (see **Figure 1O**).

3.35. Attach a sterile needle to a 1 mL insulin syringe. Insert the needle below the xiphoid process, advancing toward the left shoulder, entering the thoracic cavity through the diaphragm.

Gently draw back on the syringe to remove any residual air from the thoracic cavity (see **Figure 1P**).

3.36. Remove the tape from the mouse.

3.37. Turn off isoflurane.

3.38. Continue ventilation with 100% oxygen until the mouse appears ready to awaken.

3.39. Carefully cut the 2-0 silk suture around the mouse's snout and extubate the mouse.

3.40. Transfer the mouse to a clean cage and monitor until fully recovered. Euthanize the mouse if signs of difficulty in breathing are present.

3.41. Provide postoperative analgesia by subcutaneously injecting 10 µL (0.1 mg/kg) of buprenorphine diluted in 90 µL of sterile phosphate buffered solution (PBS).

REPRESENTATIVE RESULTS:

The steps of the surgical procedure described in this protocol are summarized and illustrated in **Figure 1**. Briefly prior to surgery, mice are anesthetized and the hair over the left thorax is removed. Mice are intubated and mechanically ventilated to enable survival upon breachment of the thoracic cavity. Soft tissue overlying the ribs is excised, and a small circular defect is created, spanning the 6th and 7th ribs. The optical window frame is inserted into the defect and its bottom side (outside of the clear aperture) is adhered to the lung tissue. The window frame is then secured with a combination of sutures and adhesive, resealing the thoracic cavity and permitting the resumption of normal breathing following extubation. When successfully implanted, the lung will adhere to the optical window (which is incorporated as part of the chest wall), with intrathoracic pressure gradients preserved. This permits comfortable survival of the mouse, enabling daily imaging up to the protocol allowance (2 weeks). Intravital imaging can then be performed through the window, as previously described for other windows[15,19,20].

For visualization of various cell types, biological structures, or cellular functional states, the procedure presented here can be performed on a wide range of mice that have either been genetically manipulated to express fluorescent proteins[21] or injected with dyes[22]. The permanent nature of the window makes it compatible with techniques for relocalization of fields of view such as photoconversion[23,24] or microcartography[17,18]. Microcartography is a triangulation technique based upon using computed transformations of coordinates of fixed fiducial marks between imaging sessions in order to predict and re-localize a region of interest. In the window created as described above, these fiducial marks are light scratches etched into the window frame (**Supplemental Figure 2**) that are easily identifiable under the microscope. This makes it possible to find the same field of view multiple times, even in otherwise unmarked tissue. **Figure 2** demonstrates the result of these techniques in a mouse where the lung vasculature has been labeled by injection of a dye-labeled high molecular weight dextran (tetramethylrhodamine 155 kD dextran) and the same micro-vasculature re-localized over 3 days.

This dextran was found to be extremely useful in evaluating transient vascular openings that are induced during periods of tumor cell intravasation[25–27]. Indeed, it has been shown that, in primary breast tumors, this high molecular weight dextran is otherwise effectively sequestered to the vasculature and does not leak into the interstitium[25]. This is in contrast to dextrans of lower molecular weight (such as 10 kD or 70 kD), which have been shown to leak from neoangiogenic vessels passively[28,29]. Meanwhile, the healthy lung vasculature has been observed to be more resistant to leakage, with dextrans >10 kD only escaping to the interstitium upon insult to the organ, such as upon exposure to exosomes[30] or viruses[31]. A variety of contrast agents also exist to measure other parameters in the lung (e.g., nuclear markers, live/dead indicators, oxidative stress reporters, blood flow velocity trackers) in addition to vascular permeability. An excellent resource cataloging them can be found in the protocol by Ueki et al.[22].

The WHRIL is a technique that is very well-suited to investigating the dynamics of blood flow in the lung. This can be accomplished in several ways. First, when imaged using relatively slow frame rates (~1–10 frames per second, fps) blood flow velocities can be determined by the shadows that unlabeled erythrocytes make when flowing in larger vessels. At low fps, these shadows form lines whose angle relative to the vessel can be used to calculate erythrocyte flow rates[32] (**Figure 2**, yellow lines). Second, shadows can also be tracked on low fps microscopes by aligning the vessels with the fast scan axis of the microscope and acquiring kymographs using rapid line scanning[33–35]. Finally, when imaging at high frame rates (>10 fps) on a microscope capable of integrating the signal over time (e.g., a spinning disk confocal equipped with a charge-coupled device (CCD) detector), individual particles can be traced directly[16,17]. In this situation, stationary objects appear as bright dots, and flowing objects trace out tracks through with the circulation. Cell speeds can be quantified by measuring the length of the tracks and dividing by the frame acquisition time. An example of this is given in **Figure 3** and **Supplemental Movie 1,** where 2 µm fluorescent microspheres have been intravascularly injected into the mouse before imaging.

With the ability to repeatedly and consistently return to the same field of view, visualization of processes that evolve over multiple days is now possible. As a demonstration of this application, the WHRIL was used to visualize the metastatic progression of breast cancer cells within the lungs[17,21]: that is, to track over time the fate of individual tumor cells that arrive at the lung vasculature. This concept is depicted in **Figure 4A**, where a single disseminated tumor cell is visualized shortly after lodging in a segment of lung micro-vasculature. Returning to that same location on subsequent days reveals the tumor cell's fate (e.g., recirculation, extravasation, etc.). Applied to the investigation of the culminating steps of metastatic progression in the lung, it was possible to visually chronicle dynamic processes, including tumor cell arrival (**Figure 4B**), extravasation (**Figure 4C**), and proliferation to form macro-metastasis (**Figure 4D**).

FIGURE AND TABLE LEGENDS:

Figure 1: Summary of surgery for the implantation of the Window for High-Resolution Imaging of the Lung (WHRIL).

Figure 2: Microcartography enables the relocalization of fixed positions within the optical window. Multiphoton intravital imaging of a single region of the lung under the optically transparent coverslip shows microvasculature relocated over 3 consecutive days using microcartography. Yellow arrows indicate a clearly definable branch point from a single vessel identified each consecutive day. Yellow lines highlight shadows that unlabeled erythrocytes make when flowing in larger vessels. The angle of these lines relative to the vessel can be used to calculate erythrocyte flow rates. Red = tdTomato labeled endothelial cells and 155 kDa Tetramethylrhodamine dextran labeled blood serum, Green = GFP labeled tumor cells, Blue = second harmonic generation. Scale bar = 15 μm.

Figure 3: Visualization of blood flow rate. Blood flow rates can be visualized by injecting 2 μm diameter fluorescent microspheres retro-orbitally and imaging their passage through the blood vessels. When imaged on a microscope capable of integrating the signal over time (e.g., a spinning disk confocal equipped with a CCD detector), stationary microspheres appear as bright dots (arrows), and flowing spheres trace out tracks through with the circulation (bracketed lines). Scale bar = 50 μm.

Figure 4. The WHRIL can capture each step of the metastatic cascade within the lung by directly visualizing the fate of disseminated tumor cells. (**A**) Tracking the fate of disseminated tumor cells (green) is achievable with serial imaging, over several days, through the WHRIL. On Day 1, a tumor cell is observed to have arrived to and lodged in the lung vasculature. On Day 2 and Day 3 the cell is no longer present in the lung vasculature, having either recirculated or died. Scale bar = 15 μm. (**B–D)** Visualization of each of the stages of tumor cell metastasis in the lung. (**B**) An intravascular disseminated tumor cell (green) lodged in the lung vasculature after arrival. (**C**) Disseminated tumor cell (green) after extravasating into the lung parenchyma. (**D**) Tumor cells that have proliferated and grown into micro-metastases. Red = tdTomato labeled endothelial cells and 155 kDa Tetramethylrhodamine dextran labeled blood serum, Green = GFP labeled tumor cells, Blue = second harmonic generation. Scale bar = 20 μm.

Supplemental Movie 1: Video corresponding to Figure 3 showing the lung vasculature with circulating 2 μm microspheres.

Supplemental Figure 1: Mechanical design drawings for the stainless-steel cutting tool used to guide the 5 mm biopsy punch.

Supplemental Figure 2: Mechanical design drawings for the stainless-steel window frame.

Supplemental Figure 3: Mechanical design drawings for the window holder tool.

DISCUSSION:

At sites of distant metastasis such as the lung, high-resolution optical imaging provides insight into the elaborate dynamics of tumor cell metastasis. By enabling *in vivo* visualization of single cancer cells and their interactions with the host tissue, high-resolution intravital imaging has proven instrumental to understanding the mechanisms underlying metastasis.

Described here is an improved surgical protocol for the permanent thoracic implantation of an optical window designed to enable serial imaging of the murine lung via high-resolution multiphoton microscopy. The window created using this protocol is well-tolerated and, given its ability to successfully reseal the thoracic cavity, is able to maintain the intrathoracic pressure gradients necessary for spontaneous ventilation (contrary to any other previously described window for imaging of the murine lung[14–16,36,37]). This permits the mouse to awaken from anesthesia, breathe independently, and comfortably survive with the transparent ribcage for an extended period of time spanning multiple weeks.

Using this window, it was possible to visualize, with single-cell resolution, all of the steps of metastasis, including arrival, extravasation, and growth into micrometastases.

Although the protocol requires some technical proficiency, with practice and careful attention to several key steps, the procedure can be performed with a high success rate. First, when removing hair prior to surgery, it is critical to protect the mouse's skin by removing the depilatory cream a moistened tissue after no more than 20 s of contact. During surgery, extreme caution should be paid to avoid cutting vessels. Excessive bleeding, most commonly encountered due to the division of either the brachial or internal mammary arteries during removal of the mammary fat pad, can obscure visualization in the surgical field or lead to death through exsanguination. Newly described in this protocol is the utilization of a biopsy punch and cutting tool (**Supplemental Figure 1**), which considerably hasten and simplify the creation of the circular defect through the rib cage and a window holder tool making implantation easier. The implementation of these advances significantly improves the success rate of the procedure and reduces the required level of prior surgical skill. Individual laboratories can use the drawings in the supplemental figures to manufacture these tools with either in-house or commercial machine shops. An internet search for "machine shop bidding sites" will yield several online applications that will aid in finding local commercial machine shops.

Finally, it is crucial to ensure that the lung tissue remains dry before adhesive application. The most common pitfall resulting in unsuccessful coverslip attachment is failure to ensure complete removal of moisture from the lung surface prior to apposition with the frame or cover glass. Furthermore, to ensure quality images, an extremely thin layer of glue (<10 μm) should be applied. Excess glue should be scraped off prior to placement of the cover glass.

The main limitation of IVI through the WHRIL is the relatively limited depth of penetration achievable. Therefore, pathology occurring deep within the lung is inaccessible. Despite this limitation, the technique can still yield an abundance of clinically relevant information, especially in oncologic investigations, given the described proclivity for peripherally localized lung metastases[38–41]. Ultimately, this imaging approach provides a considerable advantage over standard *ex vivo* assays and other methods for *in vivo* imaging, which either disconnect tissue from vital physiological processes[10–13], or limit longitudinal analysis to a maximum duration of 12 h[14–16,37,42], respectively.

For repeated imaging over this time period, several challenges must still be overcome. First, it is important to maintain the health of the skin around the implanted window, for, while the wounded tissue is not exposed, the skin around may still become inflamed or infected. Routine application of an antibiotic ointment will help prevent this. Second, with time, exudate from the cut skin may congeal under the window frame and prevent the placement of the fixturing plate used to immobilize the mouse in the microscope stage. Placing a wet tissue over the WHRIL for 10–15 min will soften this exudate and allow placement of the window frame. Third, one of the body's mechanisms for excreting excess water and maintaining homeostasis is via exhalation of vapor. Thus, too much fluid intake (mostly as a result of injection of contrast agents or tumor cell suspensions) will cause the lung surface to excrete this excess water and will result in the lung tissue detaching from the WHRIL. This can be avoided by limiting the volume of injections to a maximum of 50 µL at a time. Finally, even with the best of care, lung tissue may occasionally detach from the WHRIL due to the mouse ingesting a large volume of water or due to the mouse overexerting itself. When this occurs, detachment of the lung tissue from the WHRIL typically occurs slowly, starting at the outside edge. Thus, it may be impossible to follow some fields of view located on the first day of imaging for the full duration of the window. It was found that the best imaging results will be obtained within the first few days and that employing mosaicking techniques such as the previously published Large-Volume High-Resolution Intravital Imaging[21] can minimize the impact of this limitation.

Given that the WHRIL is integrated into the chest wall of the mouse, drift during imaging is generally not a significant issue, as long as care is paid to ensure that the attachment between the window and the microscope is firm. Still, some small amount of drift may be observed during the time immediately following placement of the mouse in the microscope stage. This may come from the relaxation of the mouse's body or from the thermal expansion of the microscope components (stage plate, XY stage, objective lens) due to the environmental chamber. This drift may be avoided by allocating ~30 min for equilibration before starting the imaging procedure. This period of time allows the mouse's physiology to stabilize under the anesthesia and allows all components to come to thermal equilibrium. Any small amount of residual drift may easily be handled by computational algorithms such as StackReg[43] or HyperStackReg[44].

Finally, this protocol is an improvement over the prior written version for two reasons. First, the visual format allows a better conceptualization of the surgical protocol. This is particularly useful for the crucial steps where 1) the lung is dried by applying a steady gentle stream of compressed air (step 3.24, **Figure 1J**), 2) the coverslip is attached to the window frame's central bore in a way that prevents entrapment of bubbles (step 3.31), and 3) a small amount of liquid cyanoacrylate is added at the metal-glass interface to ensure an air-tight seal between the coverglass and the window frame (step 3.34, **Figure 1O**).

In conclusion, with the advent of the WHRIL, given its amenability to subcellular visualization of the same lung tissue across an extended period, investigators are newly empowered to address many unanswered questions. Specifically, the protocol outlined herein enables fundamental exploration of the dynamic processes underlying numerous pathologies, including the progression of cancer metastasis.

ACKNOWLEDGMENTS:

This work was supported by the following grants: CA216248, CA013330, Montefiore's Ruth L. Kirschstein T32 Training Grant CA200561, METAvivor Early Career Award, the Gruss-Lipper Biophotonics Center and its Integrated Imaging Program, and Jane A. and Myles P. Dempsey. We would like to thank the Analytical Imaging Facility (AIF) at Einstein College of Medicine for imaging support.

DISCLOSURES:

The authors disclose no conflicts of interest.

REFERENCES:

1. Mehlen, P., Puisieux, A. Metastasis: a question of life or death. *Nature Reviews Cancer*. **6** (6), 449–458 (2006).
2. Lee, Y. T. Breast carcinoma: pattern of metastasis at autopsy. *Journal of Surgical Oncology*. **23** (3), 175–180 (1983).
3. Chambers, A. F., Groom, A. C., MacDonald, I. C. Dissemination and growth of cancer cells in metastatic sites. *Nature Reviews Cancer.* **2** (8), 563–572 (2002).
4. Coste, A., Oktay, M. H., Condeelis, J. S., Entenberg, D. Intravital imaging techniques for biomedical and clinical research. *Cytometry Part A*. **95** (5), 448–457 (2019).
5. DeClerck, Y. A., Pienta, K. J., Woodhouse, E. C., Singer, D. S., Mohla, S. The tumor microenvironment at a turning point knowledge gained over the last decade, and challenges and opportunities ahead: A white paper from the NCI TME network. *Cancer Research*. **77** (5), 1051–1059 (2017).
6. Borriello, L. et al. The role of the tumor microenvironment in tumor cell intravasation and dissemination. *European Journal of Cell Biology*. **99** (6), 151098 (2020).
7. Hosseini, H. et al. Early dissemination seeds metastasis in breast cancer. *Nature*. **540** (7634), 552–558 (2016).
8. Harper, K. L. et al. Mechanism of early dissemination and metastasis in Her2(+) mammary cancer. *Nature*. **540** 589–612 (2016).
9. Risson, E., Nobre, A. R., Maguer-Satta, V., Aguirre-Ghiso, J. A. The current paradigm and challenges ahead for the dormancy of disseminated tumor cells. *Nature Cancer*. **1** (7), 672–680 (2020).
10. Qian, B. et al. A distinct macrophage population mediates metastatic breast cancer cell extravasation, establishment and growth. *PLoS One*. **4** (8), e6562 (2009).
11. Qian, B. Z. et al. CCL2 recruits inflammatory monocytes to facilitate breast-tumour metastasis. *Nature*. **475** (7355), 222–225 (2011).
12. Miyao, N. et al. Various adhesion molecules impair microvascular leukocyte kinetics in ventilator-induced lung injury. *American Journal of Physiology-Lung Cellular and Molecular Physiology*. **290** (6), L1059–1068 (2006).
13. Bernal, P. J. et al. Nitric-oxide-mediated zinc release contributes to hypoxic regulation of pulmonary vascular tone. *Circulation Research*. **102** (12), 1575–1583 (2008).
14. Entenberg, D. et al. In vivo subcellular resolution optical imaging in the lung reveals early metastatic proliferation and motility. *IntraVital*. **4** (3), 1–11 (2015).

15. Rodriguez-Tirado, C. et al. Long-term High-Resolution Intravital Microscopy in the Lung with a Vacuum Stabilized Imaging Window. *Journal of Visualized Experiments: JoVE*. **116**, 54603 (2016).
16. Looney, M. R. et al. Stabilized imaging of immune surveillance in the mouse lung. *Nature Methods*. **8** (1), 91–96 (2011).
17. Entenberg, D. et al. A permanent window for the murine lung enables high-resolution imaging of cancer metastasis. *Nature Methods*. **15** (1), 73–80 (2018).
18. Dunphy, M. P., Entenberg, D., Toledo-Crow, R., Larson, S. M. In vivo microcartography and subcellular imaging of tumor angiogenesis: a novel platform for translational angiogenesis research. *Microvascular Research*. **78** (1), 51–56 (2009).
19. Harney, A. S., Wang, Y., Condeelis, J. S., Entenberg, D. Extended time-lapse intravital imaging of real-time multicellular dynamics in the tumor microenvironment. *Journal of Visualized Experiments: JoVE*. **112**, e54042 (2016).
20. Seynhaeve, A. L. B., Ten Hagen, T. L. M. Intravital microscopy of tumor-associated vasculature using advanced dorsal skinfold window chambers on transgenic fluorescent mice. *Journal of Visualized Experiments: JoVE*. **131**, 55115 (2018).
21. Entenberg, D. et al. Time-lapsed, large-volume, high-resolution intravital imaging for tissue-wide analysis of single cell dynamics. *Methods*. **128**, 65–77 (2017).
22. Ueki, H., Wang, I. H., Zhao, D., Gunzer, M., Kawaoka, Y. Multicolor two-photon imaging of in vivo cellular pathophysiology upon influenza virus infection using the two-photon IMPRESS. *Nature Protocols*. **15** (3), 1041–1065 (2020).
23. Ritsma, L., Ponsioen, B., van Rheenen, J. Intravital imaging of cell signaling in mice. *IntraVital*. **1** (1), 2–10 (2012).
24. Kedrin, D. et al. Intravital imaging of metastatic behavior through a mammary imaging window. *Nature Methods*. **5** (12), 1019–1021 (2008).
25. Harney, A. S. et al. Real-time imaging reveals local, transient vascular permeability, and tumor cell intravasation stimulated by TIE2hi macrophage-derived VEGFA. *Cancer Discovery*. **5** (9), 932–943 (2015).
26. Karagiannis, G. S. et al. Assessing tumor microenvironment of metastasis doorway-mediated vascular permeability associated with cancer cell dissemination using intravital imaging and fixed tissue analysis. *Journal of Visualized Experiments: JoVE*. **148**, 59633 (2019).
27. Karagiannis, G. S. et al. Neoadjuvant chemotherapy induces breast cancer metastasis through a TMEM-mediated mechanism. *Science Translational Medicine*. **9** (397) (2017).
28. Dreher, M. R. et al. Tumor vascular permeability, accumulation, and penetration of macromolecular drug carriers. *Journal of the National Cancer Institute*. **98** (5), 335–344 (2006).
29. Rizzo, V., Kim, D., Duran, W. N., DeFouw, D. O. Ontogeny of microvascular permeability to macromolecules in the chick chorioallantoic membrane during normal angiogenesis. *Microvascular Research*. **49** (1), 49–63 (1995).
30. Hoshino, A. et al. Tumour exosome integrins determine organotropic metastasis. *Nature*. **527** (7578), 329–335 (2015).
31. Ueki, H. et al. In vivo imaging of the pathophysiological changes and neutrophil dynamics in influenza virus-infected mouse lungs. *Proceedings of the National Academy of Sciences of the United States of America*. **115** (28), E6622–E6629 (2018).

32. Kornfield, T. E., Newman, E. A. Measurement of retinal blood flow using fluorescently labeled red blood cells. *eNeuro*. **2** (2) (2015).
33. Dasari, S., Weber, P., Makhloufi, C., Lopez, E., Forestier, C. L. Intravital microscopy imaging of the liver following leishmania infection: An assessment of hepatic hemodynamics. *Journal of Visualized Experiments: JoVE*. **101**, e52303 (2015).
34. Chaigneau, E., Roche, M., Charpak, S. Unbiased analysis method for measurement of red blood cell size and velocity with laser scanning microscopy. *Frontiers in Neuroscience*. **13**, 644 (2019).
35. Kim, T. N. et al. Line-scanning particle image velocimetry: an optical approach for quantifying a wide range of blood flow speeds in live animals. *PLoS One*. **7** (6), e38590 (2012).
36. Presson, R. G., Jr. et al. Two-photon imaging within the murine thorax without respiratory and cardiac motion artifact. *American Journal of Pathology*. **179** (1), 75–82 (2011).
37. Tabuchi, A., Mertens, M., Kuppe, H., Pries, A. R., Kuebler, W. M. Intravital microscopy of the murine pulmonary microcirculation. *Journal of Applied Physiology*. **104** (2), 338–346 (2008).
38. Travis, W. D. Classification of lung cancer. *Seminars in Roentgenology*. **46** (3), 178–186 (2011).
39. Scholten, E. T., Kreel, L. Distribution of lung metastases in the axial plane. A combined radiological-pathological study. *Radiologica Clinica (Basel)*. **46** (4), 248–265 (1977).
40. Braman, S. S., Whitcomb, M. E. Endobronchial metastasis. *Archives of Internal Medicine*. **135** (4), 543–547 (1975).
41. Herold, C. J., Bankier, A. A., Fleischmann, D. Lung metastases. *European Radiology*. **6** (5), 596–606 (1996).
42. Kimura, H. et al. Real-time imaging of single cancer-cell dynamics of lung metastasis. *Journal of Cellular Biochemistry*. **109** (1), 58–64 (2010).
43. Thevenaz, P., Ruttimann, U. E., Unser, M. A pyramid approach to subpixel registration based on intensity. *IEEE Transactions on Image Processing: A Publication of the IEEE Signal Processing Society*. **7** (1), 27–41 (1998).
44. Sharma, V. P. ImageJ plugin HyperStackReg V5.6. *Zenodo.* doi:10.5281/zenodo.2252521 (2018).

Figure 1

Click here to access/download;Figure;Slide1.TIF

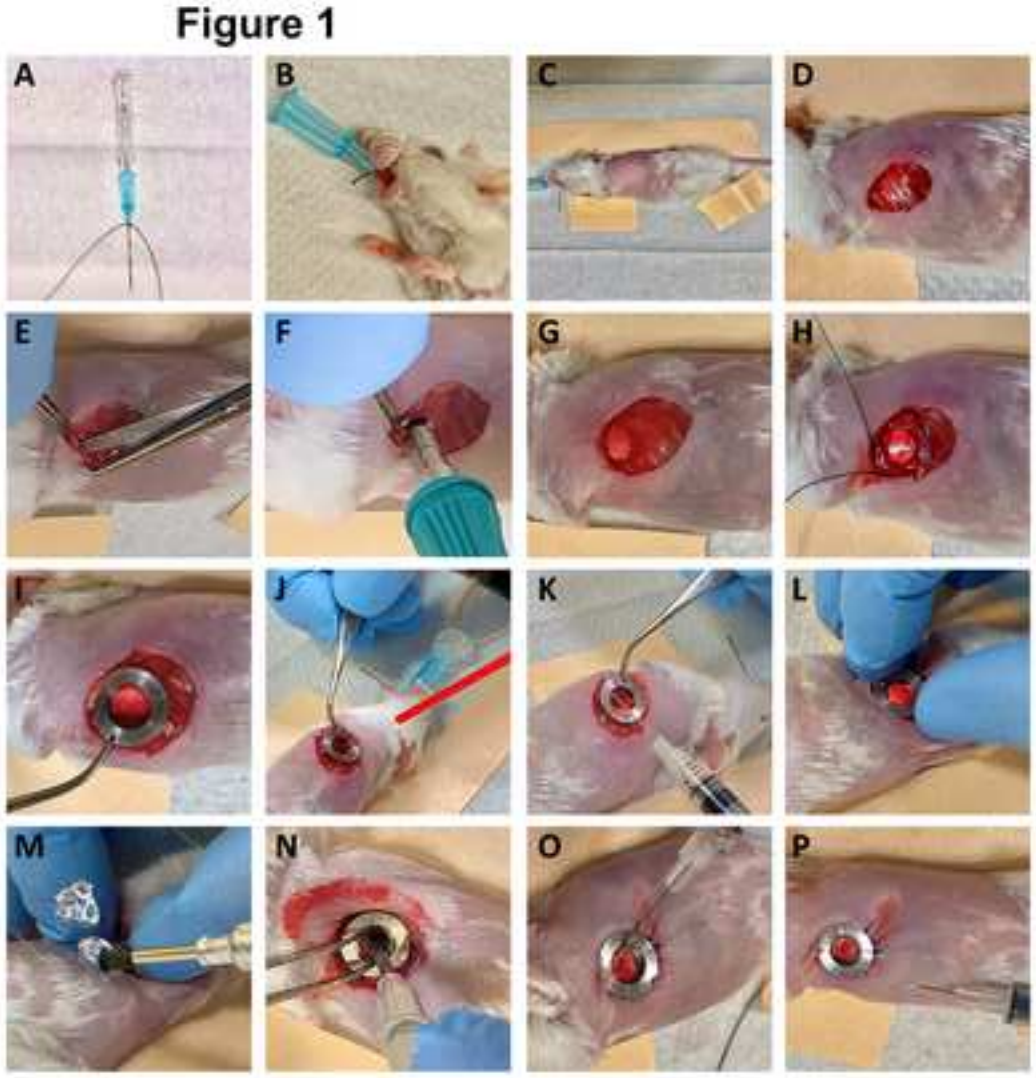

Figure 2

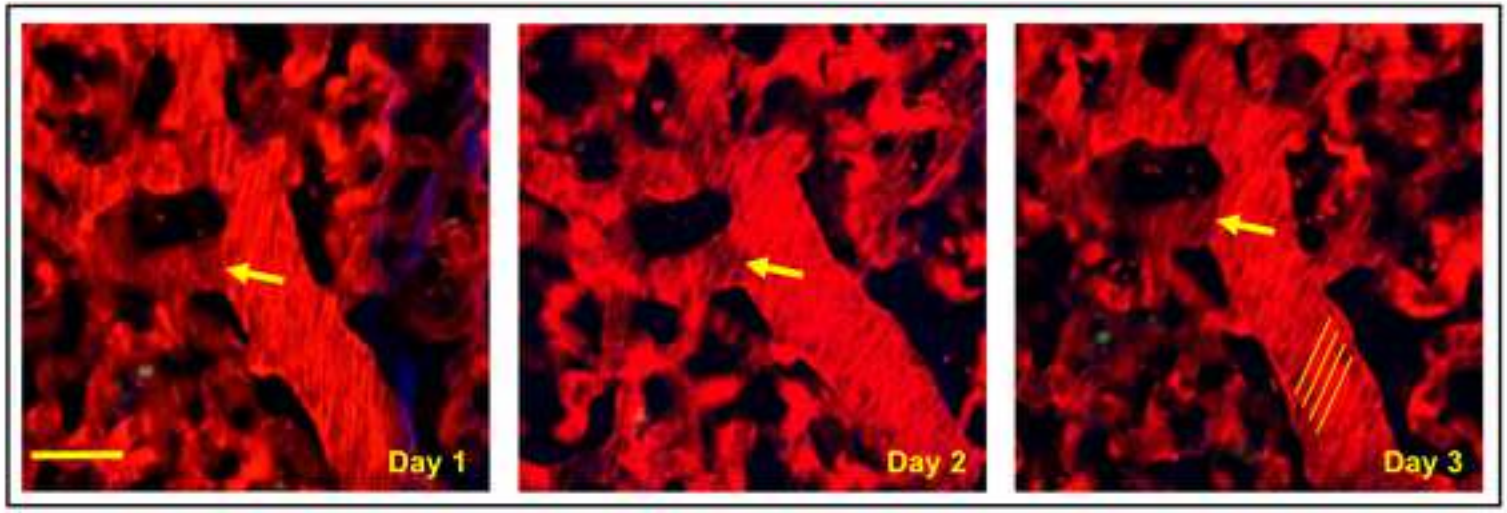

Figure 3

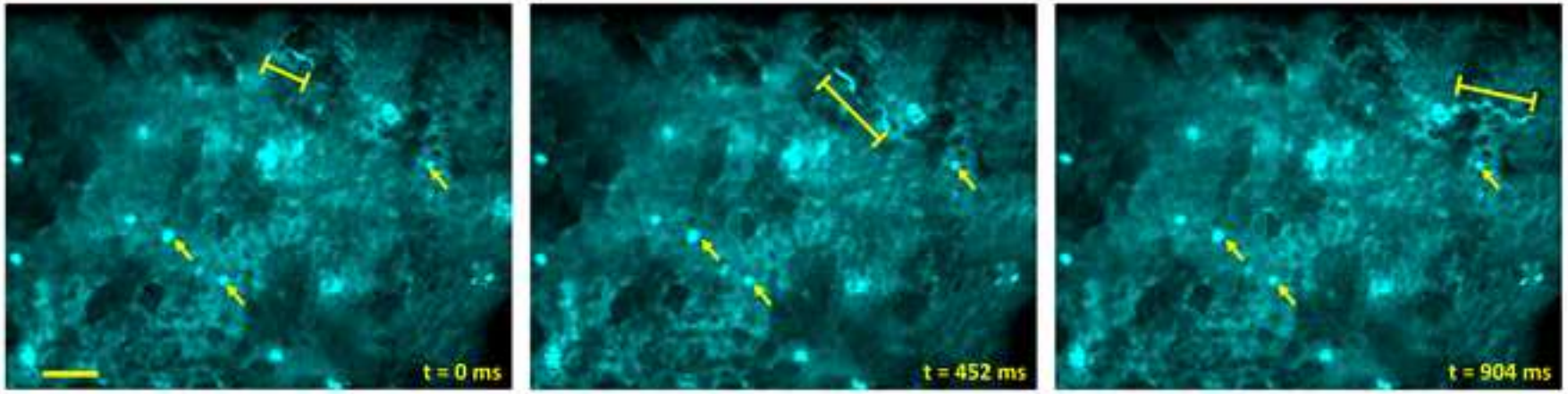

Figure 4

Click here to access/download;Figure;Slide5.TIF

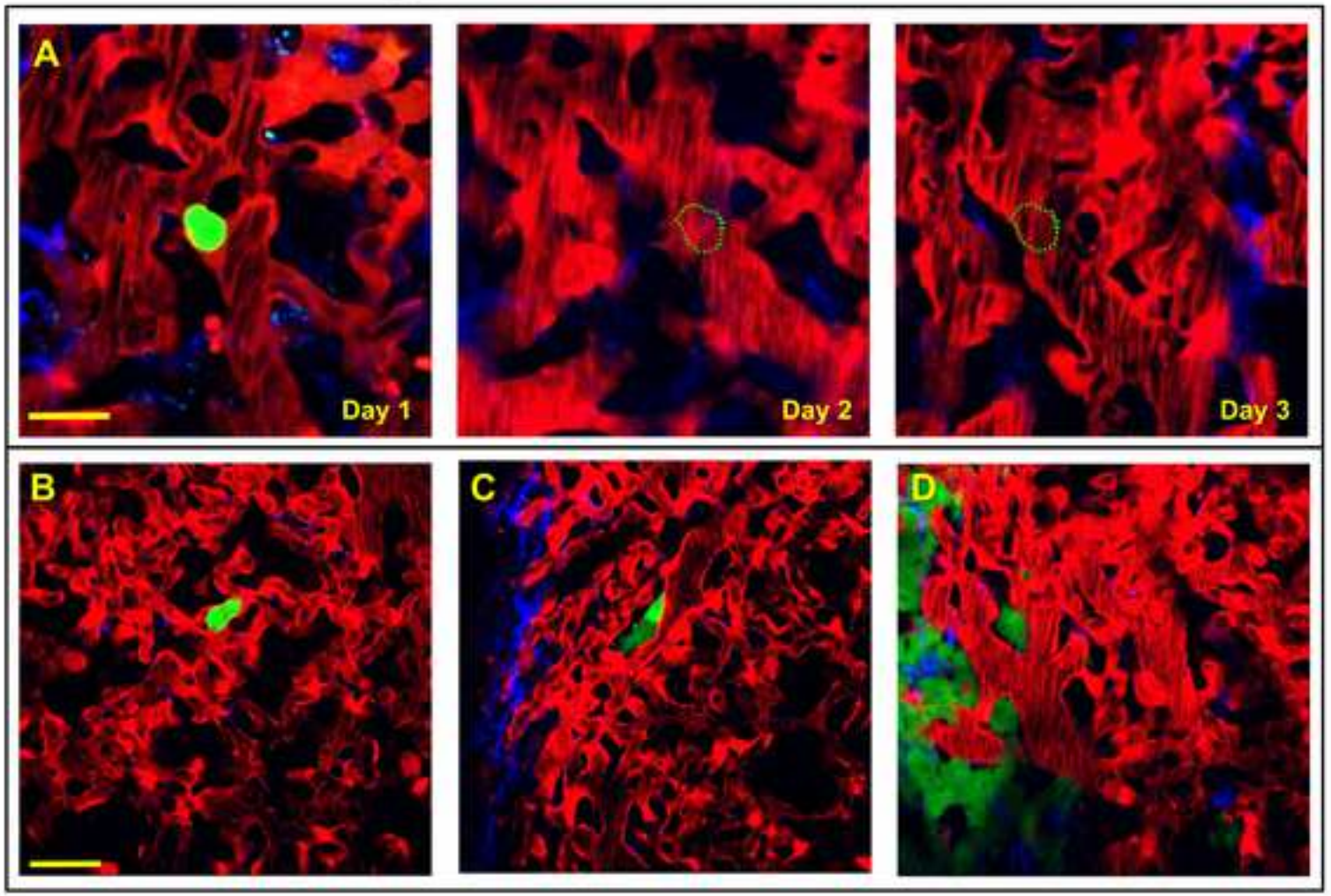

Supplemental Figure 1

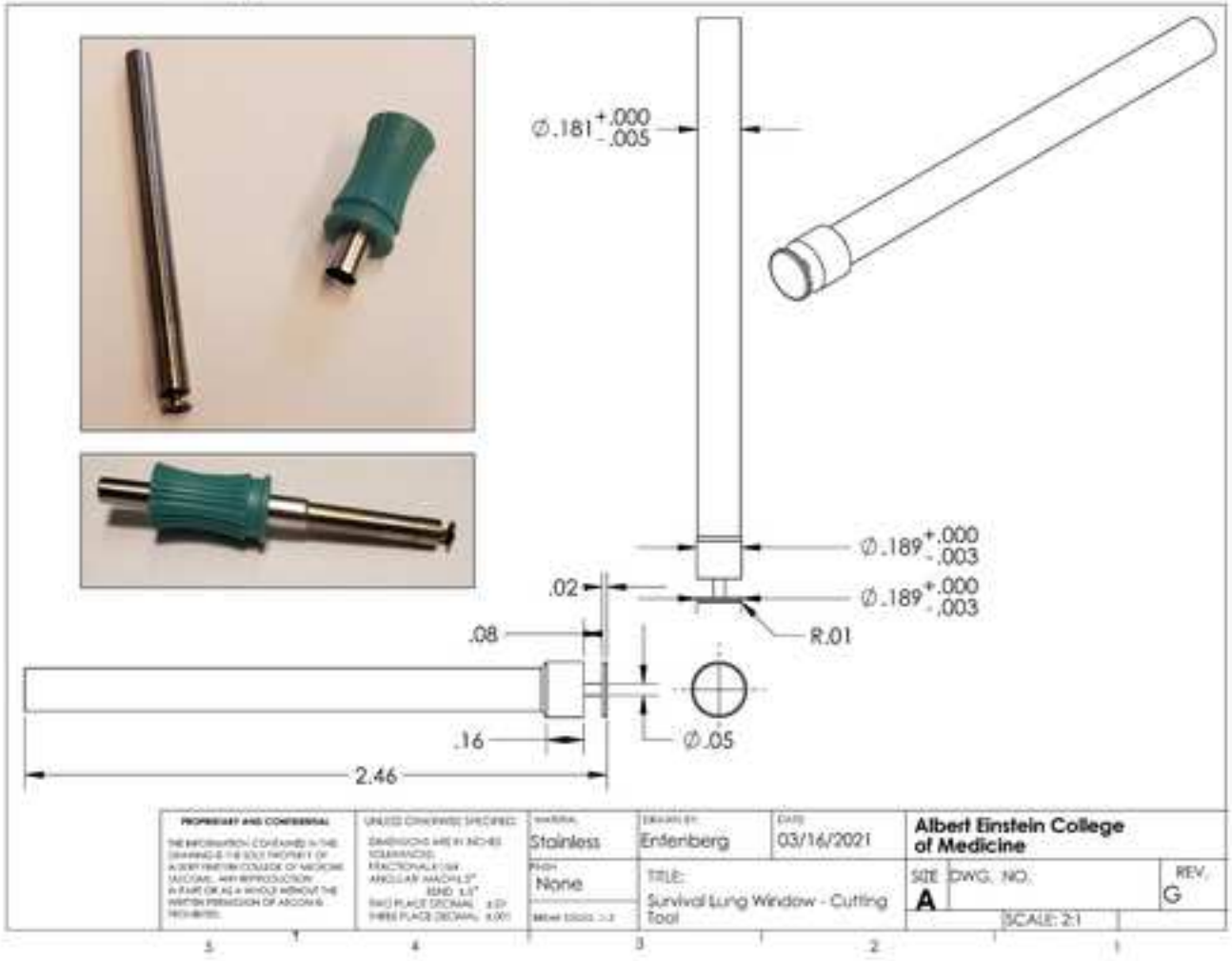

Supplemental Figure 2

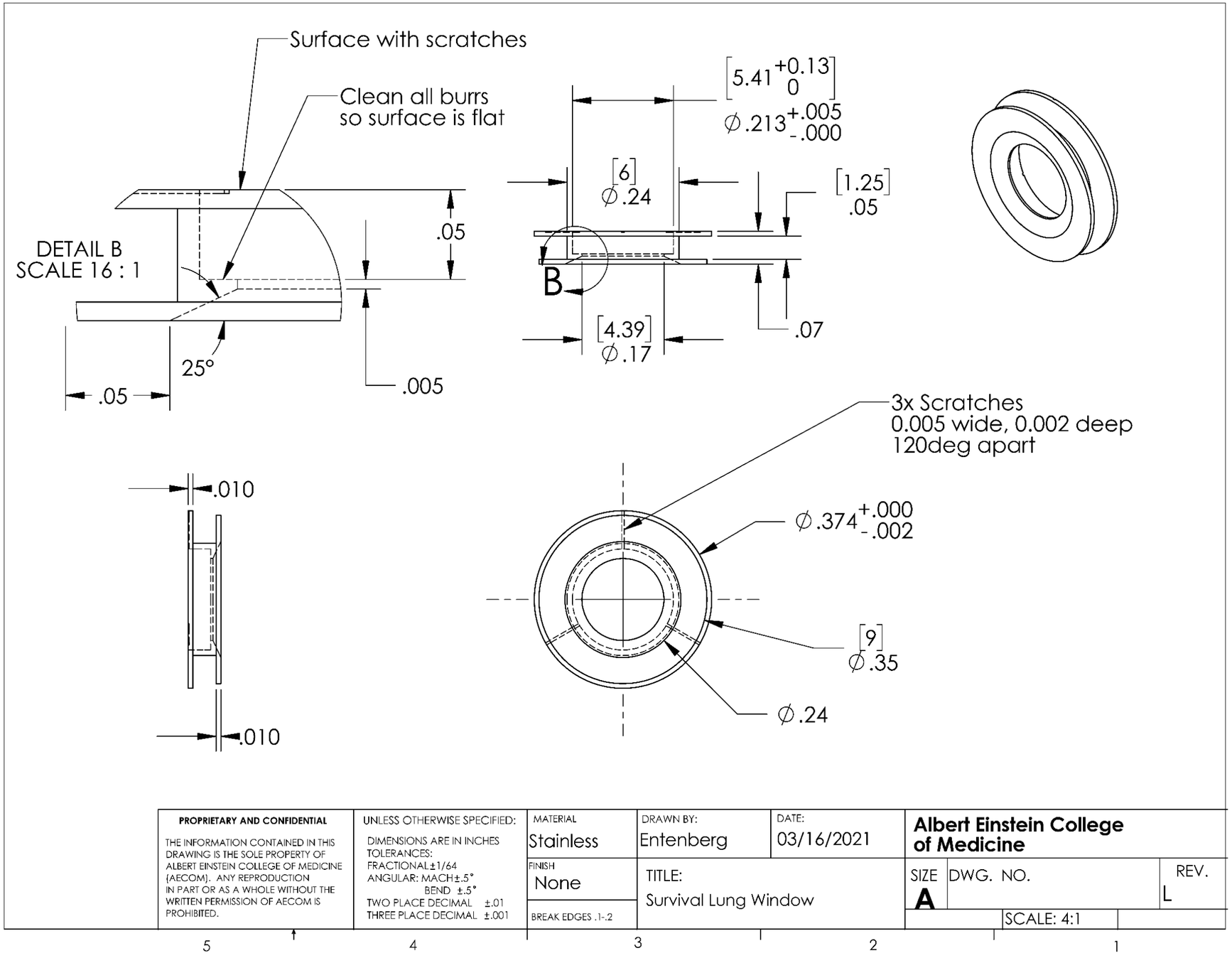

Supplemental Figure 3

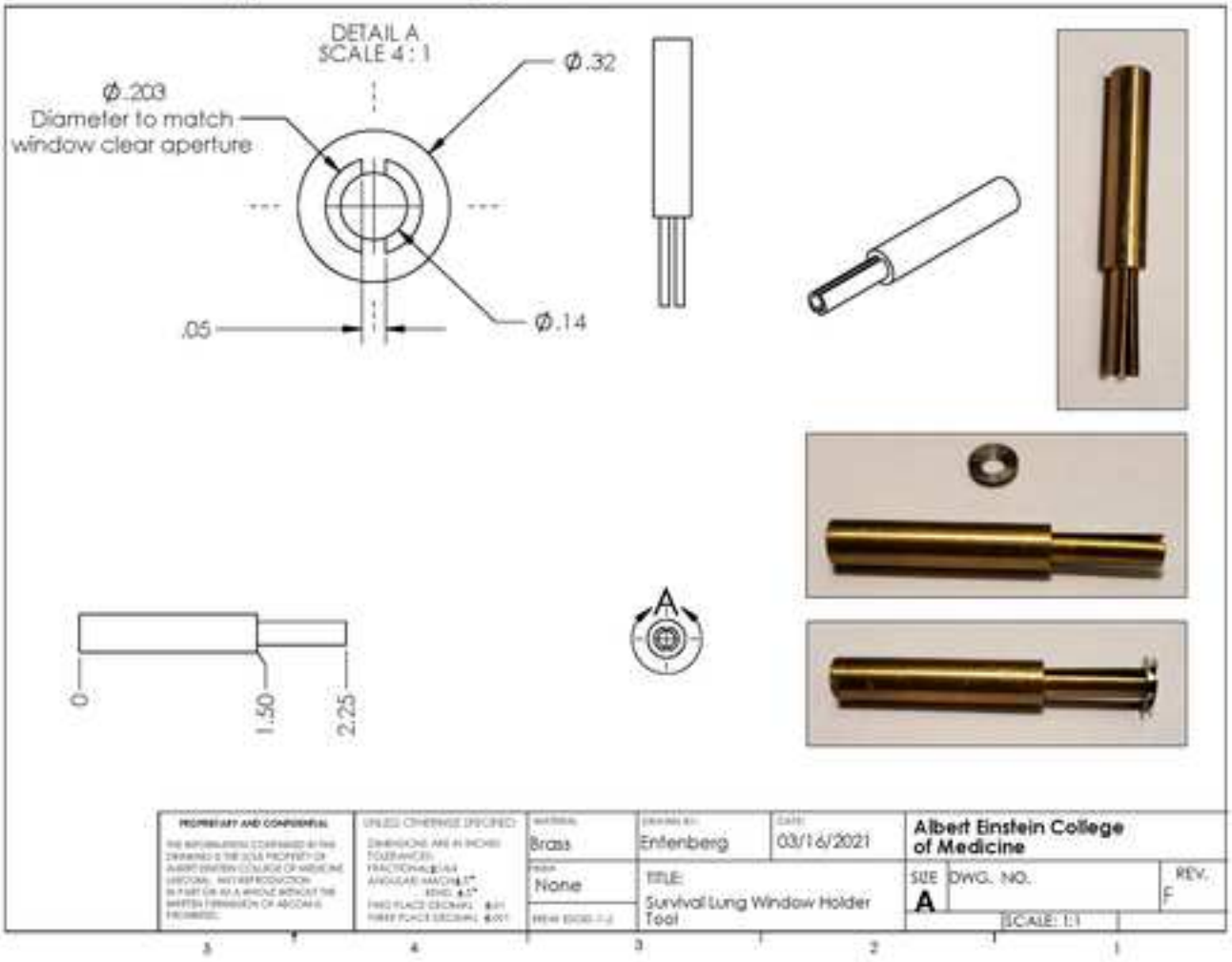

Video or Animated Figure

Click here to access/download

Video or Animated Figure

M1-06 - Pos3 Low Speed - Slow.mp4

Click here to access/download

Table of Materials

Table of Materials_62761-R1.xlsx

JoVE submission JoVE62761

A Permanent Window for Investigating Cancer Metastasis to the Lung

Rebuttal letter

We want to thank the reviewers for taking time to review of our manuscript and for their pertinent comments. We are happy to have been able to address all of their critiques in the attached revised manuscript. We have listed their comments below followed by our response in blue.

Editorial comments:

Changes to be made by the Author(s):

1. Please take this opportunity to thoroughly proofread the manuscript to ensure that there are no spelling or grammar issues. Please define all abbreviations at first use.

Response. We edited the manuscript and believe we have caught all spelling and grammar issues and defined all abbreviations at first use.

2. Please provide an email address for each author.

Response. We have provided the email addresses for each author on the title page.

3. Please add a Summary to clearly describe the protocol and its applications in complete sentences between 10-50 words: “Here, we present a protocol to …”

Response. We have included a new summary paragraph on the title page.

4. Please revise the following lines to avoid overlap with previously published work: 26-28, 46-48, 69-70, 139-140, 165-166, 182-185, 189-190, 200-202, 204-205, 294-297, 306-309, 321-322.

Response. We have indicated the lines in question in green font and have revised them. We have also made numerous other language changes to avoid overlap.

5. JoVE cannot publish manuscripts containing commercial language. This includes trademark symbols (™), registered symbols (®), and company names before an instrument or reagent. Please remove all commercial language from your manuscript (text, figure legends, figures, tables) and use generic terms instead. All commercial products should be sufficiently referenced in the Table of Materials and Reagents. For example: Vacuum Pick-Up System etc

Response. We have removed all commercial language from the manuscript.

6. Please use SI units: h not hrs.

Response. We have corrected the abbreviations.

7. For in-text formatting, corresponding reference numbers should appear as numbered superscripts after the appropriate statement(s), but before punctuation.

Response. We have adjusted the positioning of the references and made them all superscripts.

8. Please remove the reagents and equipment from the text (lines 100 to 140) and move them into the Table of Materials, which should contain the essential supplies, reagents, and equipment. The table should include the name, company, and catalog number of all relevant materials in separate columns in an xls/xlsx file. Please sort the Materials Table alphabetically by the name of the material.

Response. We have removed the reagents and equipment from the text and placed them in the Materials table.

9. Please ensure that all text in the protocol section is written in the imperative tense as if telling someone how to do the technique (e.g., “Do this,” “Ensure that,” etc.). The actions should be described in the imperative tense in complete sentences wherever possible. Avoid usage of phrases such as “could be,” “should be,” and “would be” throughout the Protocol. Any text that cannot be written in the imperative tense may be added as a “Note.” However, notes should be concise and used sparingly. Please include all safety procedures and use of hoods, etc.
Response. We have modified the written style as requested.

10. Please note that your protocol will be used to generate the script for the video and must contain everything that you would like shown in the video. Please ensure you answer the “how” question, i.e., how is the step performed? Alternatively, add references to published material specifying how to perform the protocol action. There should be enough detail in each step to supplement the actions seen in the video so that viewers can easily replicate the protocol.
Response. We have made sure the question “how” is answered for each step.

11. Please format the manuscript as: paragraph Indentation: 0 for both left and right and special: none, Line spacings: single. Please include a single line space between each step, substep and note in the protocol section. Please use Calibri 12 points and one-inch margins on all the side. Please include a ONE LINE space between each protocol step and then HIGHLIGHT up to 3 PAGES of protocol text for inclusion in the protocol section of the video.
Response. We have formatted the manuscript as indicated and highlighted the protocol text for inclusion in the video.

12. Please move the legends section to appear between the representative results and the discussion sections.
Response. We have moved the legends section.

13. Please ensure that the references appear as the following: [Lastname, F.I., LastName, F.I., LastName, F.I. Article Title. Source (ITALICS). Volume (BOLD) (Issue), FirstPage–LastPage (YEAR).] For 6 and more than 6 authors, list only the first author then et al. Please include volume and issue numbers for all references, and do not abbreviate the journal names.
Response. We have modified the references.

Reviewer #1:

This is an excellent manuscript, which reports in detail the protocol for setting-up permanent windows for longitudinal imaging in mice. Given the emergence of intravital imaging for in vivo studies of pathophysiology, this work is very timely and of interest to the readership of JoVE. The manuscript is well written and the figures and movies are of excellent quality.

Major Concerns:

No major concerns.

Minor Concerns:

Given that most intravital imaging studies will require blood vessel staining, more details on how to best use dextran conjugates are necessary. The materials could be listed in the reagent list. Also, what concentrations are recommended and whether repeated injection is necessary (if so, how often). A short paragraph on how the authors recommend to best process time-course lung imaging data to minimise drifting (due to the breathing, etc) would be helpful to most readers.

Response. We have added the dextran dye used in this study to the Reagents table . We have also included a brief paragraph on the use of dextran conjugates and other contrast agents (line 300 of the revised manuscript) in the lung. Additionally, we included a short paragraph on how to minimize drift. (line 450 of the revised manuscript).

Reviewer #2:

Boriello et al., demonstrate how to place a WHRIL for single cell resolution imaging of lung. Their protocol is well written and directions are clear. This will be definitely very useful for many scientists in the field.

Major Concerns:

None

Minor Concerns:

1. On step 40, is the glue applied to the undersurface of the optical window frame gluing the frame and the exposed lung tissue or the frame and the muscle?

Response. The glue is applied to the undersurface of the optical window frame gluing the frame and the exposed lung tissue outside of the clear aperture. We clarify this point in line 277 in the revised manuscript.

2. The engineering schematics are nice to have but it would be useful for the reader to have up close pictures of the custom-made tools from different angles.

Response. We have included close up pictures of the custom-made tools in their respective supplemental figures.

3. Given the proprietary nature of the custom tool design, can the authors comment on the best way to obtain such tools? Would it be through contacting the authors and getting permission to manufacture or would they be made by their institution as a service?

Response. We have included details on how these parts may be manufactured on line 410 of the revised manuscript.

4. Can the authors please highlight the major differences between this protocol and their published work in ref (16)?

Response. In the discussion, we included a short paragraph describing the major differences between this protocol and our previously published work (line 461 of the revised manuscript).

5. The authors mention that the imaging sessions can extend to several weeks. What are some of the obstacles that prevent the utility of the WHRIL beyond several weeks? Does the frame get loose? Does the frame get infected? What are some of the signs that the readers should watch out for the well being of the mice and imaging quality.

Response. There are several challenges in performing imaging sessions over several weeks. We have detailed these in the manuscript on line 430 of the revised manuscript.